RSC Applied Polymers

ROYAL SOCIETY OF CHEMISTRY

PAPER

View Article Online
View Journal | View Issue

Check for updates

Cite this: *RSC Appl. Polym.*, 2024, **2**, 905

Vitrimerization of crosslinked poly(ethylene-vinyl acetate): the effect of catalysts†

Amin Jamei Oskouei, [a] Erqian Mao,[b] Thomas G. Gray, [b] Alireza Bandegi,[a] Sarah Mitchell, [c] Michelle K. Sing, [c] Jayme Kennedy,[c] Kimberly Miller McLoughlin [c] and Ica Manas-Zloczower*[a]

Received 26th March 2024,
Accepted 7th July 2024

DOI: 10.1039/d4lp00112e

rsc.li/rscapplpolym

Over the past decade, research interest has grown rapidly in covalent adaptable networks, called vitrimers, which can balance the processability and recyclability of thermoplastics with the performance properties of thermosets, including elastomers. While most vitrimer research focuses on generating new materials, several studies have demonstrated that permanently crosslinked networks can be transformed into covalent adaptable networks through a mechanochemical process. This finding points to an effective and efficient technical approach for upcycling waste thermoset plastics. Recent studies have demonstrated that crosslinked ethylene vinyl acetate (EVA) thermosets can be converted to vitrimers using a mechanochemical process employing a zinc-catalyzed transesterification reaction. The concept has been applied successfully to vitrimerize crosslinked EVA elastomers and foams, including shoe midsole foam, which is otherwise difficult to recycle. To investigate whether catalyst selection could be used to control the crosslink exchange kinetics and network properties of the vitrimers produced, we compare the effects of different zinc catalysts on the vitrimerization of crosslinked EVA elastomers. We use a computational chemistry approach to select zinc catalysts with different small molecule activation energies and then apply these catalysts to vitrimerize crosslinked EVA. We find that the flow activation energies measured by experiments for the dynamic network exchanges are markedly different from the activation energies predicted by simulation for small molecule exchange. Our results suggest that the dynamic exchange rates of vitrimerized crosslinked EVA elastomers depend not only on the activation barrier for small molecule exchange but also on catalyst physical properties such as the molecular size and stability at the processing temperature.

Introduction

Vitrimer chemistry has gained attention in the past decade as a potential solution to the growing plastic waste crisis.[1,2] The inclusion of reversible crosslinks can facilitate polymer recycling and promote a circular economy. Initially, vitrimers were synthesized by incorporating reversible chemistries into polymer backbones during polymerization or *via* post-reactor modifications.[3–6] The first targeted vitrimer synthesis by Leibler and co-workers was of epoxy resins crosslinked by labile zinc carboxylates.[3] Recently, Manas and co-workers have introduced the concept of vitrimer chemistry to polymer networks already containing permanent crosslinks. This vitrimerization process converts permanent covalent crosslinks into crosslinks with dynamic moieties to generate a vitrimer. In previous work, crosslinked networks containing an ester moiety were converted into a vitrimer by embedding a crosslink exchange (transesterification) catalyst into the network by solvent swelling or agitation in a planetary or cryo-ball mill.[7–12] These vitrimer networks were reprocessable upon heating through multiple cycles without significant loss of mechanical properties. The vitrimerization process was first demonstrated in epoxy-anhydride thermosets and has been demonstrated more recently for crosslinked ethylene-vinyl acetate (EVA) elastomers.[13]

There is a broad range of dynamic chemistries used to produce vitrimer networks, for example transesterification is a well-established and robust industrial chemistry.[14,15] Transesterification reactions are often catalyzed with a catalyst, and the type and concentration of catalyst used are known to influence the reaction rate and the exchange rate of the reversible network.[16–18] Commonly used transesterification catalysts

[a]*Department of Macromolecular Science and Engineering, Case Western Reserve University, 10900 Euclid Avenue, Cleveland, OH 44106, USA. E-mail: ixm@case.edu*
[b]*Department of Chemistry, Case Western Reserve University, 10900 Euclid Avenue, Cleveland, OH 44106, USA*
[c]*Braskem America, 550 Technology Drive, Pittsburgh, PA 15219, USA*
† Electronic supplementary information (ESI) available. See DOI: https://doi.org/10.1039/d4lp00112e

include Lewis acids and nucleophiles that are metal complexes with hemilabile ligands.[14,19–21] For example, zinc-based catalysts are common transesterification catalysts used in producing ester-based vitrimers as zinc enhances the electrophilicity of an ester carbonyl, making it more susceptible to nucleophiles and promoting transesterification.[14,22–24] Zinc-based catalysts have long been attractive choices in the synthesis of vitrimers.[16,25–29]

With a wide range of effective catalysts available for transesterification in vitrimers, catalyst selection is important depending on the desired application. Recent work suggests that screening for vitrimerization catalysts can be mechanistically guided.[14,30,31] To select an appropriate catalyst, density-functional theory (DFT) is an effective computational approach to predict the activation energy of bond exchange by transesterification.[13] For example, transesterification within vitrimers is often modeled using a small molecule reaction based on the nucleophilic acyl transfer mechanism (Scheme 1).[32] This mechanism is supported by the observed isotopic oxygen-exchange in ester hydrolysis.[33,34]

In our previous work, we demonstrated that permanently crosslinked EVA networks can be transformed into vitrimers using zinc acetate as the transesterification catalyst. Zinc functions as an internal transesterification catalyst that mediates dynamic exchange between crosslinked or free vinyl acetate functionalities and feedstock alcohol.[13] The resulting material is a dynamically crosslinked network that behaves as a thermoset at low temperatures but flows as a thermoplastic elastomer at higher temperatures. The associative nature of this dynamic exchange process maintains the number density of crosslinks within the network.

In this work, we continue to explore the vitrimerization of crosslinked EVA focusing on the effects of different zinc catalysts on the exchange dynamics of the vitrimer using a combination of computational chemistry and experiments. DFT calculations are used to calculate the activation energy of the associative exchange of carbon, which is believed to be the dominant contributor to stress relaxation in networks with dynamic transesterification chemistries. Experimental measurements of stress relaxation are used to characterize vitrimers that are produced through a mechanochemical process with zinc catalysts with different anions. We find that the calculated activation energy for small molecule exchange can be used to predict the ability to form a vitrimer network. However, the activation energy predicted by computational chemistry only partially describes the exchange dynamics and relaxation behavior of crosslinked vitrimer networks. Other factors, including crosslink density, influence the observed relaxation behavior of vitrimerized EVA networks.

Experimental section

Materials

EVA was supplied by Braskem with 21.8 wt% vinyl acetate content. High molecular weight poly(vinyl alcohol), PVOH (M_w = 130 000 g mol^{-1}), dicumyl peroxide (DCP), zinc acetate, zinc stearate and zinc(II) acetylacetonate were purchased from Sigma-Aldrich and used as received. Zinc trifluoroacetate hydrate was purchased from Fisher Scientific and used as received.

Compounding and crosslinking EVA

The mixing of DCP with EVA pellets was performed in a micro-compounder (Xplore) in flush mode at a screw speed of 30 rpm and all temperature zones were held constant close to the melting temperature of EVA (100 °C). The extrudate strand was chopped into small pieces (3–5 mm) and fed into the micro-compounder for a second pass. The crosslinking of EVA/DCP blends was performed using compression molding (Carver press) at 175 °C for 15 minutes under a constant pressure of 1 MPa. The molds were 1 mm thick. The properties of EVA[35] and the molar feed ratio are reported in Table S1.† Following the crosslinking process, a stress relaxation test on crosslinked EVA was performed at 110 °C, showing no relaxation, which indicates the presence of a highly crosslinked network (Fig. S1†).

Vitrimerization process

The fine crosslinked EVA particles (<1 mm) were cryo-milled with the catalyst and alcohol in a cryogenic ball-mill tank (Retsch Cryomill). All components were dried for 24 hours and the tank was purged using N_2 (g) prior to cryo milling. The concentration of the catalyst was kept constant at 8 mol% relative to the vinyl acetate (VA) content (Table 1). The concentration of feedstock hydroxyl groups (PVOH) was kept constant at a 1.5 molar ratio of hydroxyl to VA groups ([OH]/[VA] = 1.5). The cryomilled powders (<200 μm, 1.5–2 gram) were vitrimer-

Table 1 Amount of catalyst and alcohol used for the vitrimerization of EVA

Catalyst	Abbreviation	M_w (g mol^{-1})	PVOH (wt%)	Catalyst (wt%)
Zinc acetate	$Zn(OAc)_2$	183.48	13.9	3.1
Zinc(II) acetylacetonate	$Zn(acac)_2$	263.61	13.7	4.4
Zinc trifluoroacetate hydrate	$Zn(TFA)_2$	291.42	13.7	4.8
Zinc stearate	$Zn(St)_2$–9.8 wt%	632.33	12.9	9.8

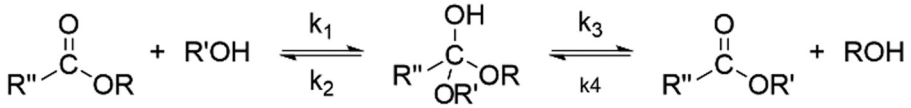

Scheme 1 Transesterification mechanism *via* a hemiketal intermediate.

ized through compression molding at 175 °C and 27 MPa with 10 minutes of preheating and 15 minutes of heating and applying pressure in the mold. The FTIR results confirm the successful vitrimerization of EVA and the formation of a metal–ligand complex (around 1580 cm^{-1}) and/or a decrease in hydroxyl peaks (a broad peak around 3300 cm^{-1}) (Fig. S2†). The details of the processing conditions are explained in our previous work.[13]

Vitrimer reprocessing procedure

Reprocessing was adapted from the method outlined in our previous work.[13] The vitrimerized samples were cut into small pieces (3–5 mm) and extruded using a minilab twin screw extruder operating at 160 °C. Then, the extruded strands were cut into small pieces (3–5 mm, 0.5 gram) and compression molded at 175 °C for 15 minutes at 27 MPa. Reprocessed samples were then evaluated based on their physical appearances.

Characterization

Dynamic mechanical analysis (DMA). The dynamic mechanical test was performed using a TA Instruments Q800. The tensile mode with a strain amplitude of 0.5% (in the linear viscoelastic region) and a constant frequency of 1 Hz was used for the measurement. The temperature was increased with a scanning rate of 5 °C min^{-1} from −50 to 200 °C. At least three samples were characterized.

Fourier transform infrared spectroscopy (FTIR). FTIR measurements were performed in a spectral range of 4000–650 cm^{-1} using an Agilent Cary 630 FTIR spectrophotometer.

Rheology. A TA ARES-G2 rheometer with a 25 mm parallel plate geometry was used to measure stress relaxation. The samples, with an average thickness of 1 mm, were equilibrated for 10 minutes at the desired temperature and then a 1% strain was applied. To have better contact between the sample and the geometry, a constant normal force of 10 N was applied during the test.

Thermogravimetric analysis (TGA). TGA measurements were conducted under an oxygen atmosphere using a TA TGA 500 in two modes, isothermal at 175 °C for 25 minutes and ramping to 550 °C at a rate of 10 °C min^{-1}.

Computations

The activation energies for transesterification employing zinc-based catalysts, specifically zinc acetate, zinc acetylacetonate, and zinc hexanoate, were calculated using density functional theory. Zinc hexanoate served as an approximation of zinc stearate to approximate the electronic effect of the alkyl chain in the carboxylic acid. All DFT calculations were carried out using the Gaussian 16 quantum chemistry program at the PBE0-D3BJ/def2-TZVP[36–38] level of theory.[39] Isopropyl alcohol and isopropyl acetate were used to model the transesterification involving secondary alcohol in the crosslinked EVA. The geometries of reactants, attacking complexes, and hemiketal intermediates were optimized in the gas phase. Harmonic frequency analysis[40] confirmed that no imaginary frequency was identified in these geometries. Transition state geometries were also optimized in the gas phase, and only one imaginary frequency corresponding to the reaction coordinate was identified. The Arrhenius activation energies were calculated based on $E_a = \Delta^{\ddagger}H^{\circ} + 2RT$, where the standard activation enthalpy was obtained from frequency analysis at 298 K and 1 atm.[41]

Results and discussion

Computation

To understand the effect of catalysts in transforming crosslinked EVA into a vitrimer, DFT was used to calculate the activation energy (E_a) of the transesterification reaction mediated by four zinc catalysts with different counterions. The catalysts were zinc acetate, zinc acetylacetonate, zinc trifluoroacetate hydrate, and zinc stearate. Computations were carried out as per the methodology described above. For three of the four catalysts (zinc acetate, zinc acetylacetonate, and zinc stearate), the optimized geometries of the reactions followed the same basic mechanism, where the vinyl acetate substrate coordinates to zinc(II) by donating a lone pair electrons to the zinc in the formation of the attacking complex. Concurrently, the feedstock forms a hydrogen bond with the anionic ligand but does not directly coordinate to zinc. The alcohol and vinyl acetate substrates are positioned next to each other, aligning the alcohol's lone pair electrons with the ester's π^* orbital, so that they are poised for a nucleophilic attack. Upon the nucleophilic attack, a coupled proton transfer occurs simultaneously between the alcohol and the anion ligand. This results in the formation of a hemiketal intermediate, wherein the anion ligand receives a proton from the alcohol. The activation energies associated with these reactions are presented in Table 2, where zinc hexanoate is used as an approximation of zinc stearate. The optimized geometries can be found in Table S2.†

For these three catalysts (zinc acetate, zinc acetylacetonate, and zinc stearate), the activation energy calculated correlates with the basicity of its anion ligand.[42] Specifically, the higher pK_a of acetyl acetonate relative to acetic acid corresponds to a greater calculated activation energy. Stearic acid, with a pK_a slightly lower than that of acetic acid, is associated with a slightly lower activation energy.

Zinc trifluoroacetate, however, exhibits a different reaction mechanism than the other three catalysts (Fig. 1). The proton

Table 2 Calculated activation energies of zinc-based catalysts at 175 °C

Catalyst	E_a (kJ mol^{-1})
$Zn(OAc)_2$[a]	+84.1
$Zn(acac)_2$[b]	+101.0
$Zn(TFA)_2$[c]	+110.0
Zinc Hexanoate[d]	+83.7

[a] OAc = acetate. [b] Acac = acetylacetonate. [c] TFA = trifluoroacetate. [d] As an approximation of zinc stearate.

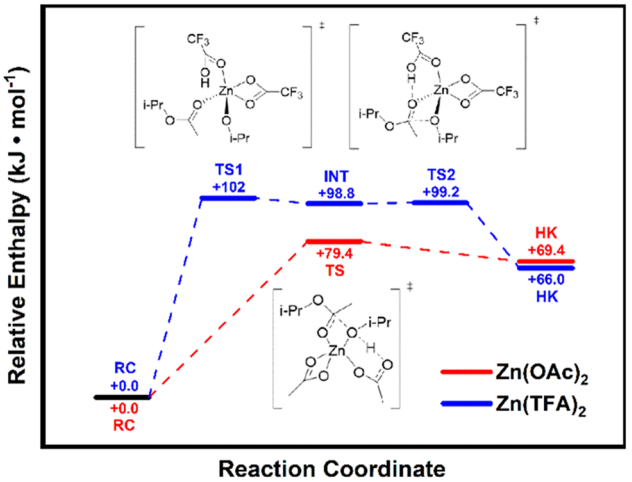

Fig. 1 DFT calculated relative enthalpy at 175 °C of concerted reaction mechanism with $Zn(OAc)_2$ *versus* stepwise reaction mechanism with $Zn(TFA)_2$. Transition state structures are shown, as they define the reaction path; the remaining structures are collected in Table S2.† RC = reactant complex; TS = transition state; INT = proton transferred intermediate; and HK = hemiketal intermediate.

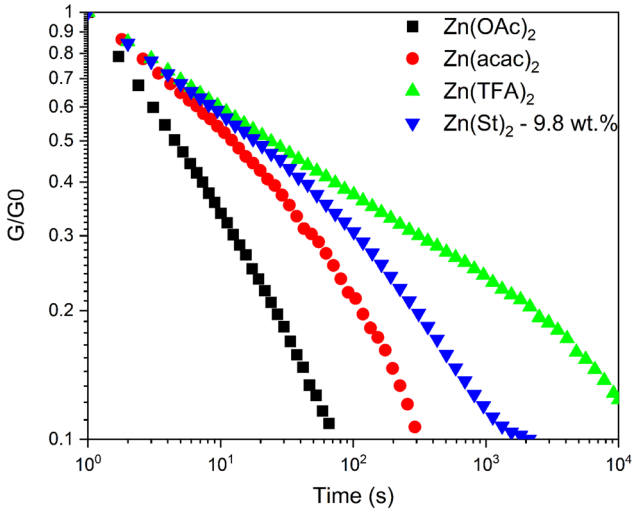

Fig. 2 Stress relaxation tests at 100 °C for $Zn(OAc)_2$, $Zn(acac)_2$, $Zn(St)_2$ and $Zn(TFA)_2$ showing a difference of behavior between the relative relaxation rates predicted by DFT and the experimental behavior.

transfer occurs prior to the nucleophilic attack, and the protonated ligand then rotates to form a hydrogen bond with the ester's carbonyl group. This rotation corresponds to the first transition state (+102 kJ mol^{-1}). The subsequent nucleophilic attack, occurring between the ester and deprotonated alcohol substrates, corresponds to the second transition state with a slightly higher energy barrier (+99.2 kJ mol^{-1}). If the small molecule activation energies act as the primary influence for network behavior, the kinetics of the reactions should decrease with increasing activation energy as follows: $Zn(St)_2$ < $Zn(OAc)_2$ < $Zn(acac)_2$ < $Zn(TFA)_2$, where $Zn(St)_2$ exhibits the fastest kinetics and thus should relax the fastest in experiments.

Flow activation energy from experiment

To further investigate the effect of the catalyst in transforming crosslinked EVA into a vitrimer, each of the four zinc catalysts was used to form a vitrimer network. At first glance, the stress relaxation behavior of the resulting networks exhibits different rates than those predicted by computation (Fig. 2). Zinc stearate, which was predicted to relax the fastest, exhibited the second slowest relaxation time, while $Zn(OAc)_2$ relaxed the fastest. However, relaxation is a temperature-dependent process. For comparison between experiment and computation, it is better to calculate the flow activation energy. The flow activation energy determines the temperature sensitivity of a process and accounts for the complex interplay between the network matrix and underlying small molecule chemistry under experimental conditions.[5,6,43] To quantify the flow activation energies of different catalysts, we utilized fitting parameters from the Kohlrausch–Williams–Watts (KWW) stretched exponential decay (Tables S3–S6†) performed at multiple temperatures. Details of the fits and calculation are included in the ESI.† The calculation of flow activation energy for each system, obtained from the slope of the Arrhenius plots (Fig. S4†), allows us to establish a comparison between the flow activation energy of each catalyst and the activation energy obtained from DFT studies (Fig. 3).

Not only does the trend in activation energy from DFT not hold, but the activation energies obtained also span a much broader range. While small-molecule DFT provides valuable information regarding the bond activation energy, it does not capture the inherent complexity of these vitrimer networks. While the DFT calculations are process-agnostic, the process required to generate the vitrimer network could impact catalyst performance. For example, zinc acetate and $Zn(acac)_2$ showed similar flow activation energies following stress relaxation

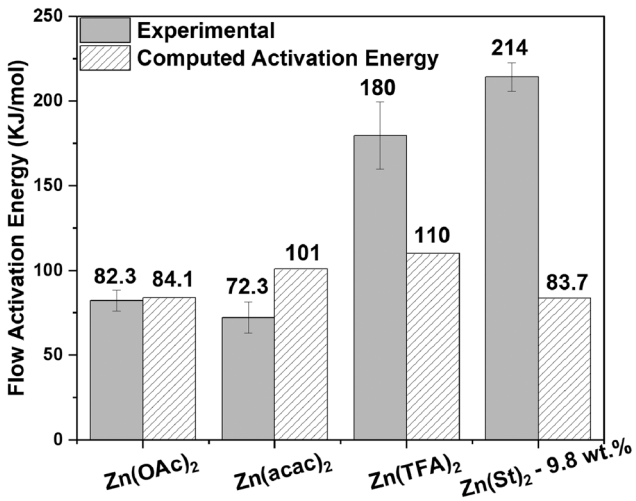

Fig. 3 Flow activation energies of various zinc salts along with their computed activation energies demonstrating the disconnect between computational and experimental studies.

experiments and $Zn(OAc)_2$ exhibited faster relaxation behavior at the same nominal temperature. However, computational studies predicted different activation energies. In order to generate vitrimer networks, it was necessary to mold at 175 °C. Thermal analysis of all four zinc salts showed that both $Zn(acac)_2$ and $Zn(TFA)_2$ lack stability at 175 °C. Both salts lose over 80 wt% of their mass in less than 15 minutes (Fig. 4). Given that the samples were molded at 175 °C for a total of 25 minutes (10 minutes of preheating and 15 minutes of compression molding), the decomposition reactions that contribute to this mass loss should be taken into consideration when choosing a catalyst system for vitrimerization and a time period that is relevant to the process used to mold the samples. Zinc acetylacetonate is known to decompose at least partially to $Zn(OAc)_2$ above 130 °C.[44,45] Given the similarities in flow activation energies between $Zn(OAc)_2$ and $Zn(acac)_2$ and the relative rates of stress relaxation provided by the lower molar concentration of $Zn(OAc)_2$ resulting from the decomposition of $Zn(acac)_2$, the decomposition of $Zn(acac)_2$ as a result of the vitrimerization process is likely the primary influence on the discrepancy between the calculated and experimental activation energies. Leibler and co-workers have observed similar catalyst concentration effects of $Zn(OAc)_2$ on the transesterification reaction.[16] When changing the concentration of the transesterification catalyst, the activation energy remains constant but the rate of the exchange reaction changes.

In the case of $Zn(TFA)_2$, decomposition is likely attributable to most of it changing into a residual substance (most likely ZnO).[46] Zinc oxide is also a transesterification catalyst, but the catalytic activity of ZnO is likely different and the resulting concentration is unknown. FTIR analysis also indicated that the mechanism for transesterification in the $Zn(TFA)_2$ samples is different from the mechanism predicted *via* DFT. The DFT calculations indicate that the Zn atom will coordinate to the O atom of the ester group (Fig. 1); however, the peak indicating this coordination does not appear at ~1580 cm^{-1} and the spectra only show a shift of the carbonyl in the trifluoroacetate group. The FTIR spectra of the vitrimer formed from the other three zinc salts show the zinc ligand formation after cryomilling as evidenced by the peak at ~1580 cm^{-1}. The lack of ligand formation with the $Zn(TFA)_2$ samples indicates that the decomposition of the catalyst is possibly changing the nature of the network formed and subsequently the flow activation energy.

However, the decomposition of the catalyst and resulting byproducts does not explain all the discrepancies between the computational activation energy and the experimental flow activation energy. Zinc stearate, much like $Zn(OAc)_2$, demonstrates minimal mass loss at 175 °C (Fig. 4), but the flow acti-

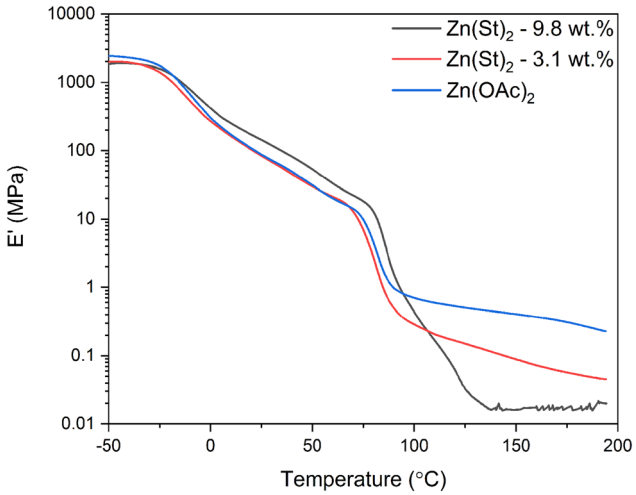

Fig. 5 DMA of $Zn(OAc)_2$ at 3.1 wt%, $Zn(St)_2$ at 9.8 wt% and $Zn(St)_2$ at 3.1 wt%, showing the lack of an elastic modulus above the melt temperature for 9.8 wt% $Zn(St)_2$. When the amount of $Zn(St)_2$ is decreased to the same amount as $Zn(OAc)_2$, the modulus demonstrates elastic network behavior. However, the lower molar ratio contributes to the modulus itself being lower for the 3.1 wt% $Zn(St)_2$ sample relative to $Zn(OAc)_2$.

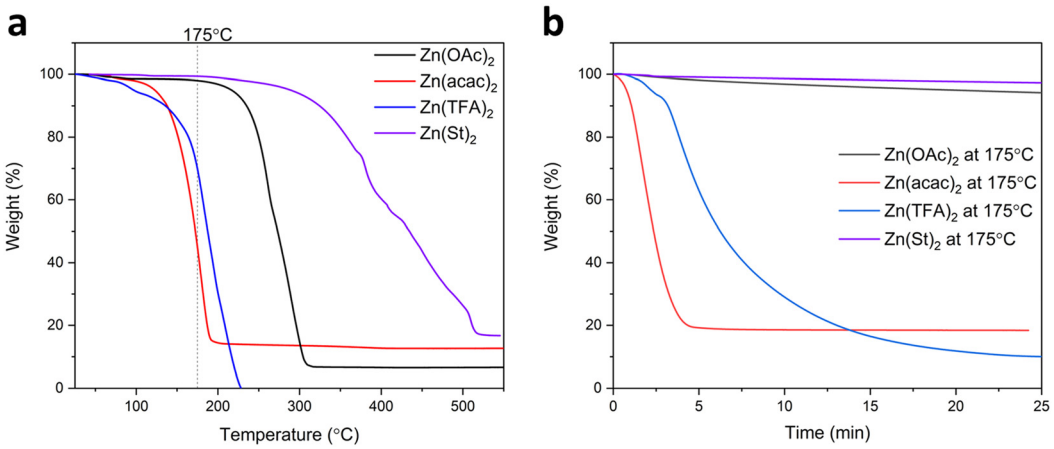

Fig. 4 TGA of pure zinc salts (a) ramped to 550 °C and (b) isothermal at 175 °C for 25 minutes. Both $Zn(acac)_2$ and $Zn(TFA)_2$ show evidence of decomposition during process relevant timescales.

vation energy from stress relaxation was much higher than the activation energy computed from DFT (Fig. 3). Furthermore, additional tests to confirm the network behavior for all four zinc salts above the melt temperature showed a sharp drop in modulus for $Zn(St)_2$ to a value that was near the lower force limit of the DMA (Fig. 5 and S5†). For purposes of comparison, the molar amount of catalyst added to create the vitrimer network was kept constant at 8 mol% relative to the amount of vinyl acetate present in the crosslinked material. For $Zn(St)_2$, this resulted in 2–3 times the amount of catalyst added to the vitrimer system by mass relative to the other zinc salts (Table 1). The high amount of catalyst (9.8 wt%) added to the system could disrupt the ability to form a network and act as more of a filler than a transesterification catalyst. The addition of fillers is reported in the literature to influence the network relaxation timescales, flow activation energy, and stiffness.[47,48] When the amount of $Zn(St)_2$ is decreased to the same amount by mass (3.1 wt%) as that of $Zn(OAc)_2$, the high temperature modulus increases, indicative of successful network formation, and the flow activation energy decreases closer to the value predicted by computation (Fig. 6). Additionally, the high temperature modulus of $Zn(St)_2$ – 3.1 wt% is roughly an order of magnitude lower than that of Zn(OAc), indicating a lower crosslink density related to the decreased molar concentration of $Zn(St)_2$.

While the higher molar mass of $Zn(St)_2$ contributes to the discrepancy between the computational activation energy and the experimental flow activation energy, it does not fully account for the difference. Counterion mobility, network inhomogeneities and the matrix are reported in the literature to influence flow activation energy and could explain the remaining differences between the calculated and experimental values for $Zn(St)_2$.[4,6,49,50]

A crucial aspect in the context of vitrimerization and catalyst selection is also the effectiveness of the catalyst in facilitating the re-processing of vitrimerized EVA. Successful reprocessing was achieved with $Zn(OAc)_2$ as demonstrated by the homogeneity of the reprocessed sample. However, for $Zn(TFA)_2$, noticeable welding lines were observed, and the samples did not attain the desired level of quality (Fig. 7). Notably, reprocessing of the sample with 9.8 wt% $Zn(St)_2$ was not pursued, as this sample did not undergo successful vitrimerization. The results of this study point to zinc acetate as an optimal catalyst for activating the transesterification reaction in crosslinked EVA vitrimerization.

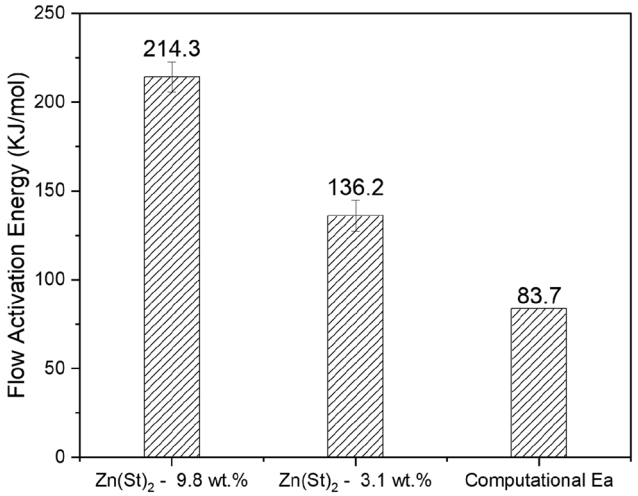

Fig. 6 Flow activation energy of $Zn(St)_2$ at high and low mass concentrations compared to the computational prediction demonstrating the influence of the amount of catalyst on the flow activation energy.

Conclusions

In this work, we use both computational and experimental methods to study the effects of catalyst selection on the vitrimerization of EVA. Specifically, we compare the effects of zinc catalysts (zinc acetate, zinc acetylacetonate, zinc trifluoroacetate hydrate, and zinc stearate) with different anions on transesterification of previously crosslinked EVA elastomers. We report the effects of catalyst selection on the kinetics of the bond exchange reaction, vitrimer thermomechanical pro-

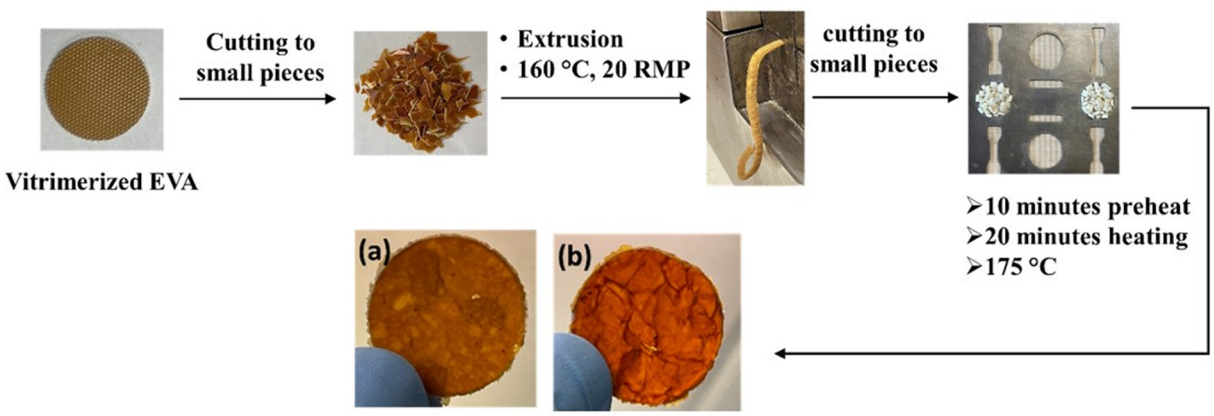

Fig. 7 Reprocessing of vitrimerized EVA prepared with (a) zinc acetate and (b) zinc trifluoroacetate.

perties, and re-processability of vitrimerized networks. Additionally, we find that the calculated activation energy for small molecule exchange can be used to predict whether a catalyst will facilitate a transesterification reaction, leading to the formulation of a vitrimerized network. However, the activation energy predicted by computational chemistry only partially describes the exchange dynamics and relaxation behavior of vitrimerized EVA networks. The physical properties of the vitrimerized EVA networks also depend on the properties of the catalyst such as the molecular size and temperature stability. Practical considerations such as thermal stability and molecular size limit the effectiveness of specific zinc catalysts. Of the catalysts that we evaluated, only zinc acetate ($Zn(OAc)_2$) demonstrates both efficient activation of the transesterification reaction and efficient reprocessing of the vitrimerized EVA.

Our findings underscore the complexity of converting previously crosslinked polymer networks into vitrimers. They point to an effective discovery process that combines computational chemistry to screen catalyst candidates with experimental methods to evaluate catalyst performance. Future work should include additional computational work to explore additional tools for better predicting the properties of vitrimers produced from previously crosslinked polymer networks.

Data availability

The data that support the findings of this study are available from the corresponding author upon reasonable request.

Conflicts of interest

CWRU and Braskem have applied for patent protection for this technology.

Acknowledgements

This work is supported by the U.S. Department of Energy's Office of Energy Efficiency and Renewable Energy (EERE) under the Advanced Materials & Manufacturing Technologies Office (AMMTO), Award Number DE-EE0007897 awarded to the REMADE Institute, a division of Sustainable Manufacturing Innovation Alliance Corp. This work made use of the High-Performance Computing Resource in the Core Facility for Advanced Research Computing at Case Western Reserve University.

References

1 J. Rajesh Banu and V. Godvin Sharmila, A systematic review on plastic waste conversion for a circular economy: Recent trends and emerging technologies, *Catal. Sci. Technol.*, 2023, **13**(8), 2291–2302.
2 J. Zheng, M. Arifuzzaman, X. Tang, X. C. Chen and T. Saito, Recent development of end-of-life strategies for plastic in industry and academia: Bridging their gap for future deployment, *Mater. Horiz.*, 2023, **10**(5), 1608–1624.
3 D. Montarnal, M. Capelot, F. Tournilhac and L. Leibler, Silica-like malleable materials from permanent organic networks, *Science*, 2011, **334**(6058), 965–968.
4 M. Guerre, C. Taplan, J. M. Winne and F. E. Du Prez, Vitrimers: Directing chemical reactivity to control material properties, *Chem. Sci.*, 2020, **11**(19), 4855–4870.
5 G. M. Scheutz, J. J. Lessard, M. B. Sims and B. S. Sumerlin, Adaptable crosslinks in polymeric materials: Resolving the intersection of thermoplastics and thermosets, *J. Am. Chem. Soc.*, 2019, **141**(41), 16181–16196.
6 B. M. El-Zaatari, J. S. A. Ishibashi and J. A. Kalow, Cross-linker control of vitrimer flow, *Polym. Chem.*, 2020, **11**(33), 5339–5345.
7 L. Yue, V. S. Bonab, D. Yuan, A. Patel, V. Karimkhani and I. Manas-Zloczower, Vitrimerization: A novel concept to reprocess and recycle thermoset waste via dynamic chemistry, *Global Challenges*, 2019, **3**(7), 1800076.
8 L. Yue, H. Guo, A. Kennedy, A. Patel, X. Gong, T. Ju, *et al.* Vitrimerization: Converting thermoset polymers into vitrimers, *ACS Macro Lett.*, 2020, **9**(6), 836–842.
9 L. Yue, M. Amirkhosravi, X. Gong, T. G. Gray and I. Manas-Zloczower, Recycling epoxy by vitrimerization: Influence of an initial thermoset chemical structure, *ACS Sustainable Chem. Eng.*, 2020, **8**(33), 12706–12712.
10 L. Yue, K. Ke, M. Amirkhosravi, T. G. Gray and I. Manas-Zloczower, Catalyst-free mechanochemical recycling of bio-based epoxy with cellulose nanocrystals, *ACS Appl. Bio Mater.*, 2021, **4**(5), 4176–4183.
11 L. Yue, M. Amirkhosravi, K. Ke, T. G. Gray and I. Manas-Zloczower, Cellulose nanocrystals: Accelerator and reinforcing filler for epoxy vitrimerization, *ACS Appl. Mater. Interfaces*, 2021, **13**(2), 3419–3425.
12 R. Rahimzadeh, Y. Han and I. Manas-Zloczower, A mechanochemical approach to recycle thermosets containing carbonate and thiourethane linkages, *Polymer*, 2024, 126877.
13 A. Bandegi, T. G. Gray, S. Mitchell, A. Jamei Oskouei, M. K. Sing, J. Kennedy, *et al.* Vitrimerization of crosslinked elastomers: a mechanochemical approach for recycling thermoset polymers, *Mater. Adv.*, 2023, **4**(12), 2648–2658.
14 J. Otera, Transesterification, *Chem Rev.*, 1993, **93**(4), 1449–1470.
15 J. Otera and J. Nishikido, Esterification: Methods, reactions, and applications, in: *Esterification: Methods, Reactions, and Applications [Internet]*, John Wiley & Sons, Ltd, 2009. p. 293–322. Available from: **https://onlinelibrary.wiley.com/doi/abs/10.1002/9783527627622.ch8**.
16 M. Capelot, M. M. Unterlass, F. Tournilhac and L. Leibler, Catalytic control of the vitrimer glass transition, *ACS Macro Lett.*, 2012, **1**(7), 789–792.
17 M. Fang, X. Liu, Y. Feng, B. Lu, M. Huang, C. Liu, *et al.* Influence of Zn^{2+}catalyst stoichiometry on curing dynamics and stress relaxation of polyester-based epoxy vitrimer, *Polymer*, 2023, **278**, 126010.

18 L. Imbernon, S. Norvez and L. Leibler, Stress relaxation and self-adhesion of rubbers with exchangeable links, *Macromolecules*, 2016, **49**(6), 2172–2178.
19 M. L. Bender, Mechanisms of catalysis of nucleophilic reactions of carboxylic acid derivatives, *Chem. Rev.*, 1960, **60**(1), 53–113.
20 J. Q. Ng, H. Arima, T. Mochizuki, K. Toh, K. Matsui, M. Ratanasak, *et al.* Chemoselective transesterification of methyl (meth)acrylates catalyzed by sodium(I) or magnesium(II) aryloxides, *ACS Catal.*, 2021, **11**(1), 199–207.
21 X. Zhao, M. Ratanasak, K. Kon, J. y. Hasegawa and K. Ishihara, Bulky magnesium(II) and sodium(I) bisphenoxide catalysts for chemoselective transesterification of methyl (meth)acrylates, *Chem. Sci.*, 2023, **14**(3), 566–572.
22 N. N. Greenwood and A. Earnshaw, *Chemistry of the Elements*, University of Leeds, Reed Educational and Professional Publishing Ltd, U.K., 2nd edn, 1997.
23 F. A. Cotton, R. A. Welch and G. Wilkinson, in *Advanced Inorganic Chemistry*, Wiley, New York, 6th edn, 1990.
24 J. Emsley, *The Elements*, Oxford University: Clarendon Press, 1980.
25 M. Capelot, D. Montarnal, F. Tournilhac and L. Leibler, Metal-catalyzed transesterification for healing and assembling of thermosets, *J. Am. Chem. Soc.*, 2012, **134**(18), 7664–7667.
26 A. Demongeot, S. J. Mougnier, S. Okada, C. Soulié-Ziakovic and F. Tournilhac, Coordination and catalysis of Zn^{2+} in epoxy-based vitrimers, *Polym. Chem.*, 2016, **7**(27), 4486–4493.
27 A. Demongeot, R. Groote, H. Goossens, T. Hoeks, F. Tournilhac and L. Leibler, Cross-linking of poly(butylene terephthalate) by reactive extrusion using Zn(II) epoxy-vitrimer chemistry, *Macromolecules*, 2017, **50**(16), 6117–6127.
28 X. Niu, F. Wang, X. Li, R. Zhang, Q. Wu and P. Sun, Using Zn^{2+} ionomer to catalyze transesterification reaction in epoxy vitrimer, *Ind. Eng. Chem. Res.*, 2019, **58**(14), 5698–5706.
29 W. Cai, Y. Huang, J. Li, G. Yang, F. Wang, G. Si, *et al.* A multifunctional biomass zinc catalyst for epoxy-based vitrimers and composites, *Eur. Polym. J.*, 2023, **188**, 111936.
30 J. M. Winne, L. Leibler and F. E. Du Prez, Dynamic covalent chemistry in polymer networks: A mechanistic perspective, *Polym. Chem.*, 2019, **10**(45), 6091–6108.
31 S. Bhusal, C. Oh, Y. Kang, V. Varshney, Y. Ren, D. Nepal, *et al.* Transesterification in vitrimer polymers using bifunctional catalysts: Modeled with solution-phase experimental rates and theoretical analysis of efficiency and mechanisms, *J. Phys. Chem. B*, 2021, **125**(9), 2411–2424.
32 M. Adler, S. Adler and G. Boche, Tetrahedral intermediates in reactions of carboxylic acid derivatives with nucleophiles, *J. Phys. Org. Chem.*, 2005, **18**(3), 193–209.
33 M. L. Bender, Oxygen exchange as evidence for the existence of an intermediate in ester hydrolysis, *J. Am. Chem. Soc.*, 1951, **73**(4), 1626–1629.
34 M. L. Bender and H. d'A. Heck, Carbonyl oxygen exchange in general base catalyzed ester hydrolysis, *J. Am. Chem. Soc.*, 1967, **89**(5), 1211–1220.
35 K. M. McLoughlin, A. Jamei Oskouei, M. K. Sing, A. Bandegi, S. Mitchell, J. Kennedy, *et al.* Thermomechanical properties of cross-linked EVA: A holistic approach, *ACS Appl. Polym. Mater.*, 2023, **5**(2), 1430–1439.
36 C. Adamo and V. Barone, Toward reliable density functional methods without adjustable parameters: The PBE0 model, *J. Chem. Phys.*, 1999, **110**(13), 6158–6170.
37 S. Grimme, J. Antony, S. Ehrlich and H. Krieg, A consistent and accurate ab initio parametrization of density functional dispersion correction (DFT-D) for the 94 elements H-Pu, *J. Chem. Phys.*, 2010, **132**(15), 154104.
38 S. Grimme, S. Ehrlich and L. Goerigk, Effect of the damping function in dispersion corrected density functional theory, *J. Comput. Chem.*, 2011, **32**(7), 1456–1465.
39 M. J. Frisch, G. W. Trucks, H. B. Schlegel, G. E. Scuseria, M. A. Robb, J. R. Cheeseman, G. Scalmani, V. Barone, G. A. Petersson, H. Nakatsuji, X. Li, M. Caricato, A. V. Marenich, J. Bloino, B. G. Janesko, R. Gomperts, B. Mennucci, H. P. Hratchian, J. V. Ortiz, A. F. Izmaylov, J. L. Sonnenberg, D. Williams-Young, F. Ding, F. Lipparini, F. Egidi, J. Goings, B. Peng, A. Petrone, T. Henderson, D. Ranasinghe, V. G. Zakrzewski, J. Gao, N. Rega, G. Zheng, W. Liang, M. Hada, M. Ehara, K. Toyota, R. Fukuda, J. Hasegawa, M. Ishida, T. Nakajima, Y. Honda, O. Kitao, H. Nakai, T. Vreven, K. Throssell, J. A. Montgomery Jr., J. E. Peralta, F. Ogliaro, M. J. Bearpark, J. J. Heyd, E. N. Brothers, K. N. Kudin, V. N. Staroverov, T. A. Keith, R. Kobayashi, J. Normand, K. Raghavachari, A. P. Rendell, J. C. Burant, S. S. Iyengar, J. Tomasi, M. Cossi, J. M. Millam, M. Klene, C. Adamo, R. Cammi, J. W. Ochterski, R. L. Martin, K. Morokuma, O. Farkas, J. B. Foresman and D. J. Fox, *Gaussian 16 (Revision B.01)*, Gaussian, Inc., Wallingford CT, 2016.
40 A. P. Scott and L. Radom, Harmonic vibrational frequencies: An evaluation of Hartree−Fock, Møller−Plesset, quadratic configuration interaction, density functional theory, and semiempirical scale factors, *J. Phys. Chem.*, 1996, **100**(41), 16502–16513.
41 D. A. McQuarrie and J. D. Simon, *Physical Chemistry: A Molecular Approach*, University Science Books, California, 1997.
42 F. G. Bordwell, Equilibrium acidities in dimethyl sulfoxide solution, *Acc. Chem. Res.*, 1988, **21**(12), 456–463.
43 A. Antoine, A. Asbai, O. Anaya, M. M. Chehimi, E. Drockenmuller and D. Montarnal, Rheological properties of covalent adaptable networks with 1,2,3-triazolium cross-links: The missing link between vitrimers and dissociative networks, *Macromolecules*, 2020, **53**, 1884–1900.
44 Y. q. Ma and Y. y. Pang, Mechanism study on char formation of zinc acetylacetonate on ABS resin, *Chin. J. Polym. Sci.*, 2015, **33**(5), 772–782.
45 G. Rudolph and M. C. Henry, The thermal decomposition of zinc acetylacetonate hydrate, *Inorg. Chem.*, 1964, **3**(9), 1317–1318.

46 Y. Zou, Y. Wang, H. Zhang, Z. Chen, J. Wang and Y. Li, Thermochemical process in preparation of ZnO film by TFA-MOD method, *Appl. Surf. Sci.*, 2007, **253**(9), 4356–4360.

47 A. M. Hubbard, Y. Ren, P. Papaioannou, A. Sarvestani, C. R. Picu, D. Konkolewicz, *et al.* Vitrimer composites: Understanding the role of filler in vitrimer applicability, *ACS Appl. Polym. Mater.*, 2022, **4**(9), 6374–6385.

48 X. Chen, L. Li, T. Wei, D. C. Venerus and J. M. Torkelson, Reprocessable polyhydroxyurethane network composites: Effect of filler surface functionality on cross-link density recovery and stress relaxation, *ACS Appl. Mater. Interfaces*, 2019, **11**(2), 2398–2407.

49 I. Alshareedah, A. Singh, S. Yang, V. Ramachandran, A. Quinn, D. A. Potoyan, *et al.* Determinants of viscoelasticity and flow activation energy in biomolecular condensates, *Sci. Adv.*, 2024, **10**(7), eadi6539.

50 R. G. Ricarte, F. Tournilhac and L. Leibler, Phase Separation and Self-Assembly in Vitrimers: Hierarchical Morphology of Molten and Semicrystalline Polyethylene/Dioxaborolane Maleimide Systems, *Macromolecules*, 2019, **52**(2), 432–443.